Heliyon 10 (2024) e27772

Contents lists available at ScienceDirect

Heliyon

journal homepage: www.cell.com/heliyon

Research article

The oncogene MYBL2 promotes the malignant phenotype and suppresses apoptosis through hedgehog signaling pathway in clear cell renal cell carcinoma

Wenjie Yang [1], Hualin Chen [1], Lin Ma [1], Mengchao Wei, Xiaoqiang Xue, Yingjie Li, Zhaoheng Jin, Jie dong [*], He Xiao [**]

Department of Urology, Peking Union Medical College Hospital, Chinese Academy of Medical Sciences and Peking Union Medical College, Dongcheng, Beijing, 100000, China

ARTICLE INFO

Keywords:
ccRCC
MYBL2
Proliferation
Apoptosis
SMO

ABSTRACT

Multiple cancers have been associated with MYB-related protein B (MYBL2), its involvement in clear cell renal cell carcinoma (ccRCC) has yet to be demonstrated. Our study revealed a significant upregulation of MYBL2 in ccRCC tissues, correlating with clinicopathological features and patient prognosis. Increased MYBL2 expression promoted cell proliferation and suppressed apoptosis. RNA-seq analysis unveiled a reduction in smoothened (SMO) expression upon MYBL2 silencing. However, luciferase and chromatin immunoprecipitation (ChIP) assays demonstrated MYBL2's positive regulation of SMO expression by directly targeting the SMO promoter. Reintroduction of SMO expression in MYBL2-knocked down cells partially restored cell proliferation and mitigated apoptosis inhibition. Overall, these results indicate that MYBL2 facilitates ccRCC progression by enhancing SMO expression, suggesting its potential as an intriguing drug target for ccRCC therapy.

1. Introduction

Renal cell carcinoma (RCC) stands out as a prevalent genitourinary cancer, representing 2-3% of all adult malignancies, with both its incidence and morbidity rate on the rise [1,2]. The most common subtype of RCC is the clear cell renal cell carcinoma (ccRCC), which accounts for 90% of all cases. At present, lymph node or distant metastases are the first signs of ccRCC in 25-30% of patients. Moreover, over 30% of patients are likely to experience a recurrence after undergoing curative surgery. This culminates in a bleak prognosis, with a five-year survival rate ranging only from 50 to 69% [3–5]. Therefore, additional efforts are needed to investigate the biological mechanisms underlying ccRCC progression.

The protein MYBL2, alternatively referred to as B-MYB, is a member of the MYB transcription factor family and is situated at the 20q13 locus. It was initially identified as a gene associated with myeloblastosis, signaling its relation to tumor growth. Acknowledged as a key gene driving cancer development, MYBL2 exhibits widespread expression in proliferating cells [6,7]. Previous research has

* Corresponding author. Department of Urology, Peking Union Medical College Hospital, Chinese Academy of Medical Sciences and Peking Union Medical College, Dongcheng, Beijing 10000, China.

** Corresponding author.

E-mail addresses: pumchdongjie@163.com (J. dong), xiaoh@pumch.cn (H. Xiao).

[1] These authors contributed equally to this work.

https://doi.org/10.1016/j.heliyon.2024.e27772
Received 27 October 2023; Received in revised form 6 March 2024; Accepted 6 March 2024
Available online 11 March 2024

clarified the crucial role of MYBL2 in cancer progression [8–10]. However, the function of MYBL2 and its molecular mechanisms within ccRCC remains relatively under-investigated.

The Hedgehog (HH) signaling pathway is a well-conserved pathway originally discovered in *Drosophila melanogaster*. It is instrumental in embryonic development, wound healing, and upholding tissue homeostasis [11,12]. While it remains primarily inactivated or minimally activated under typical physiological circumstances, anomalies in the HH signaling pathway can instigate tumorigenesis. It is also linked with aggressive cancer characteristics, including neoplastic transformation, tumor progression, metastasis, and resistance to drugs [13–15]. Thus, the HH signaling pathway stands recognized as a potential therapeutic target. The Hedgehog (HH) signaling pathway involves a variety of molecules. These include Hedgehog ligands such as the Sonic, Indian, and Desert Hedgehogs, the multi-transmembrane protein patched (PTCH) molecules like PTCH-1 and PTCH-2, smoothened (SMO) molecules, and GLI Zinc finger proteins. Out of these, SMO plays a pivotal role as a signal transducer in the HH pathway, activating downstream GLI molecules and inducing the expression of a plethora of target genes within the HH pathway. Several studies have demonstrated that aberrations in

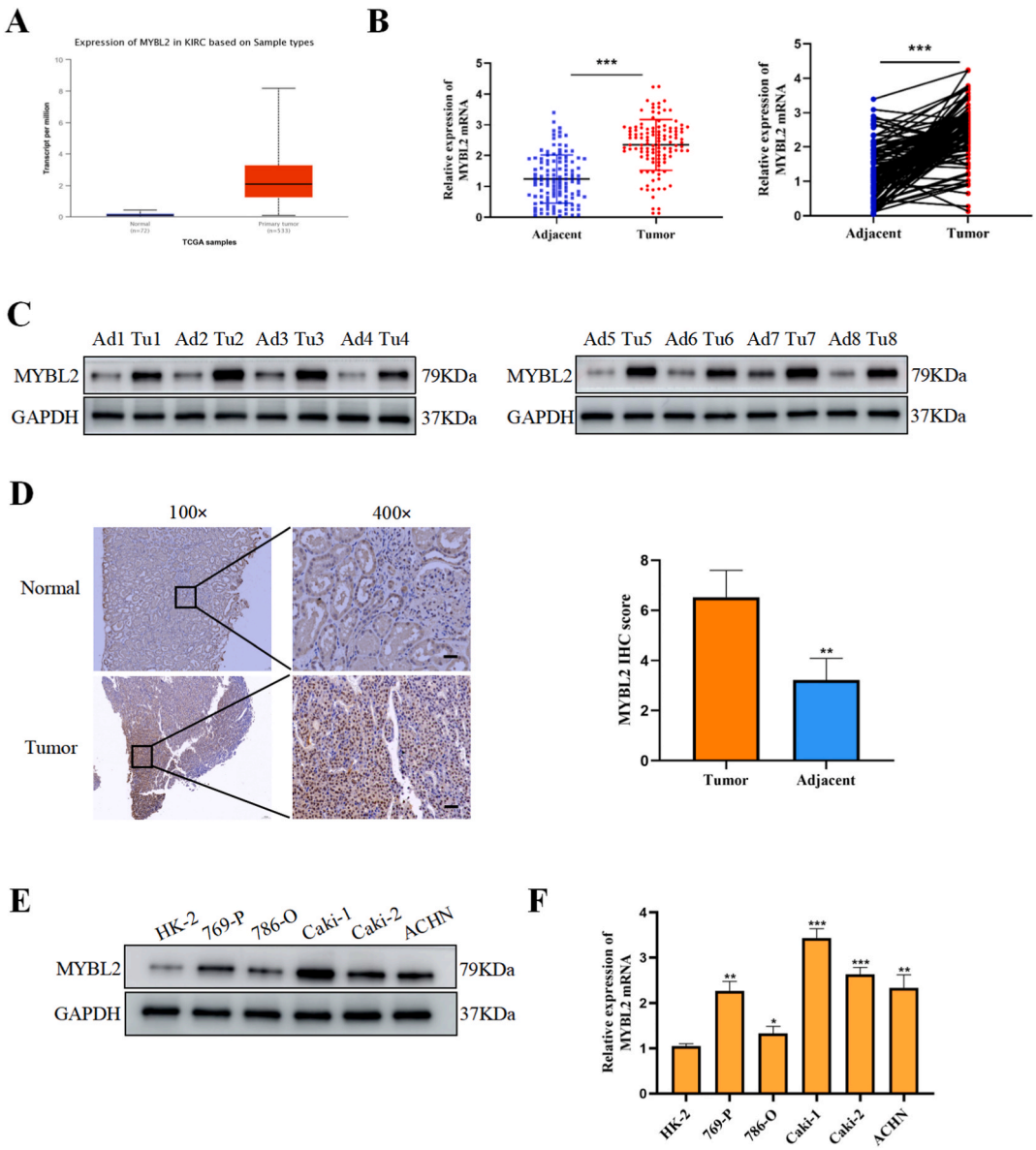

Fig. 1. MYBL2 exhibits overexpression in ccRCC. (A) Comparison of MYBL2 expression in 533 RCC tissue samples with 72 adjacent normal tissues (TCGA datasets). Analysis of MYBL2 mRNA (B) and protein (C) levels in RCC tumor tissues and corresponding adjacent nontumor tissues. (D) Representative immunohistochemical staining of MYBL2 in RCC tumor tissues compared with peritumor tissues. Scale bar = 50 μm. (E) Western blot analysis of MYBL2 expression in RCC cell lines and normal HK-2 cells. (F) Reverse transcription quantitative PCR analysis of MYBL2 expression in RCC cell lines and normal HK-2 cells. The data are presented as the mean ± standard deviation (SD) of experiments (n = 3 biological replicates). *p < 0.05, **p < 0.01, ***p < 0.001.

HH signaling can support ccRCC carcinogenesis and progression [16,17]. Nevertheless, the exact connection between MYBL2 and the HH signaling pathway remains unclear.

This study undertook a analysis of MYBL2 expression in ccRCC. Overexpression of MYBL2 was associated with reduced survival among ccRCC patients. Further mechanistic examinations elucidated the transcriptional regulatory association with the downstream gene, SMO, thereby providing a potential therapeutic target for ccRCC patients.

2. Results

2.1. MYBL2 exhibits overexpression in ccRCC

According to The Cancer Genome Atlas (TCGA) datasets, MYBL2 was significantly upregulated in primary tumor tissues. What's more, analysis of 116 surgically resected tumor tissues and paracancerous tissues from ccRCC patients revealed elevated MYBL2 expression in ccRCC (Fig. 1A, B, C). Immunohistochemical staining also revealed high *MYBL2* expression in ccRCC tissues (Fig. 1D).

Next, we evaluated MYBL2 expression in ccRCC cell lines (769-P, 786-O, Caki-1, Caki-2, and ACHN) and HK-2 cells. Our findings revealed a notable increase in MYBL2 expression across all ccRCC cell lines compared to HK-2 cells (Fig. 1E and F). 786-O cells displayed the lowest levels of MYBL2, while Caki-1 cells displayed the highest levels. Therefore, further experiments were conducted with 786-O and Caki-1 cells. These findings emphasize the substantial upregulation of MYBL2 expression in ccRCC.

2.2. Elevated MYBL2 expression is associated with an unfavorable prognosis in ccRCC patient

A threshold of 2.414 was selected in order to assess the clinical relevance of MYBL2 expression in ccRCCs by dividing patients into groups with high and low MYBL2 expression. MYBL2 expression was found to have a positive correlation with tumor size, TNM stage, and histological grade. However, no significant correlations were observed between MYBL2 expression and patient age, sex, or tumor location (Table 1). Importantly, higher *MYBL2* levels in ccRCC patients led to significantly poorer RFS and OS compared to RFS and OS of ccRCC patients with lower levels of *MYBL2* (Fig. 2A and B). Based on these data, lower *MYBL2* expression may confer a survival advantage for ccRCC patients.

2.3. MYBL2 has potent oncogenic functions in ccRCC

We employed a lentiviral approach to downregulate MYBL2 expression in Caki-1 cells and induce its overexpression in 786-O cells. Transfection efficiency was assessed using WB and qRT-PCR. In Fig. 3A and B, Caki-1 cells exhibit a significant decrease in MYBL2 expression.

MYBL2 knockdown notably decreased the viability of Caki-1 cells (Fig. 3C). Anomalously high MYBL2 expression boosted colony formation in 786-O cells, whereas MYBL2 knockdown attenuated the proliferation of Caki-1 cells (Fig. 3D). Additionally, results from EdU assays provided further validation of MYBL2's impact on ccRCC cell proliferation (Fig. 4A). Caki-1 cells were significantly suppressed by MYBL2 inhibition, while 786-O cells were significantly increased by MYBL2 overexpression. The percentage of apoptotic cells was higher in Caki-1 cells that were knocked down for MYBL2 than those in shNC cells. In contrast, *MYBL2* overexpression significantly reduced apoptosis (Fig. 4B) in 786-O cells. Based on these findings, MYBL2 promotes ccRCC cell proliferation

Table 1
Association between MYBL2 expression and clinicopathologic features of patients in RCC.

Clinicopathological indexes	MYBL2 expression		χ2	P value
	High	Low		
All cases	55	61		
Age (years)			0.091	0.927
≤60	23	25		
> 60	32	36		
Gender			1.391	0.164
Male	31	42		
Female	24	19		
Laterality			0.344	0.732
Left	27	28		
Right	28	33		
Tumor size (cm)			2.066	**0.039***
≤7	21	35		
>7	34	26		
TNM staging			2.209	**0.027***
I + II	16	30		
III + IV	39	31		
Histological Grade			3.306	**<0.001***
I-II	25	46		
III-IV	30	15		

*indicates $p < 0.05$.

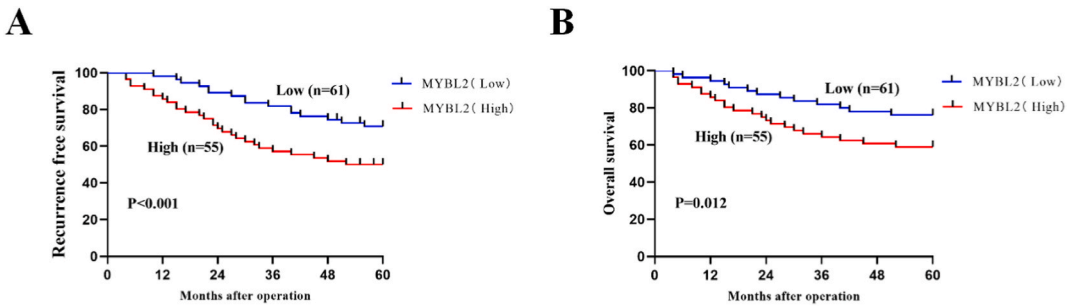

Fig. 2. Elevated MYBL2 expression is associated with an unfavorable prognosis in ccRCC patient. Kaplan–Meier curves of RFS (A) and OS (B) of RCC patients based on MYBL2 expression levels. *p < 0.05, **p < 0.01, ***p < 0.001.

and inhibits apoptosis.

2.4. Hedgehog signaling pathway is involved in the function of MYBL2

To identify the underlying mechanisms that lead to biological functions in cell proliferation and apoptosis induced by *MYBL2*, next-generation sequencing (NGS) was performed in *MYBL2*-knockdown and negative control Caki-1 cells (Fig. 5A). Subsequent to the silencing of MYBL2, there emerged 67 differentially expressed genes (DEGs) which saw an upregulation, and 298 DEGs experienced a decrease (Fig. 5B). The Kyoto Encyclopedia of Genes and Genomes (KEGG) analysis demonstrated that alterations in representative DEGs were enriched in the Hedgehog signaling pathway (Fig. 5C and D).

SMO plays a crucial role as a signal transducer in the Hedgehog pathway, influencing cell apoptosis, migration, and invasion, particularly in ccRCC [18]. For a deeper comprehension of the relationship between MYBL2 and SMO, we conducted qRT-PCR to investigate the expression profiles of SMO in ccRCC samples. Correlation analysis results revealed positive associations between MYBL2 and SMO expression in ccRCC patients (Fig. 5E).

2.5. SMO expression was regulated by the MYBL2

To explore the mechanisms behind MYBL2-induced ccRCC progression, we examined the expression patterns of SMO. MYBL2 overexpression led to a reduction in SMO level (Fig. 6A and B). Furthermore, Moreover, Gli1, a crucial factor downstream of SMO, demonstrated elevated in cells that overexpressed MYBL2, while it was significantly diminished in cells with silenced MYBL2 expression. Next, we predicted the MYBL2 binding site using the JASPAR database. (Fig. 6C and D). The luciferase assay showed a significant increase in luciferase activity of the SMO-WT promoter upon co-transfection with MYBL2. However, mutating the MYBL2 binding site to CDCA3 resulted in a notable decrease in this activation effect (Fig. 6E). Further validation was performed using a ChIP assay to confirm MYBL2's binding to the SMO promoter (Fig. 6F). Collectively, these findings indicate that MYBL2 positively modulates SMO expression by directly interacting with the SMO promoter.

2.6. MYBL2 influenced ccRCC proliferation and apoptosis by transactivating SMO

To explore the involvement of SMO in the tumor-promoting actions of MYBL2 in ccRCC, SMO-overexpression plasmid was used to increase SMO expression in MYBL2-knockdown Caki-1 cells, whereas specific siRNAs were used to silence SMO in MYBL2-overexpressing 786-O cells. As shown in Fig. 7A–C, in MYBL2-knockdown Caki-1 cells, increased SMO expression significantly promoted cell proliferation, while silencing SMO inhibited proliferation in 786-O cells (Figs. S1A–C). By flow cytometry, it was shown that SMO restored expression in MYBL2-knockdown Caki-1 cells reduced the cell apoptosis rate (Fig. 7D), while SMO knockdown led to the opposite effects (Fig. S1D). In addition, WB assays showed the restoration of SMO expression in MYBL2-knockdown Caki-1 cells decreased the expression of Bcl-2, whereas Bax expression was increased (Fig. 7E). However, silencing SMO in MYBL2-overexpressing 786-O cells produced the opposite effect. (Fig. S1E). These findings indicate that MYBL2 influenced ccRCC proliferation and apoptosis by transactivating SMO.

2.7. MYBL2 upregulation contributed to ccRCC progression in vivo

To further explore the potential contribution of MYBL2 to tumor cell growth, Caki-1 and 786-O cells were subcutaneously implanted into the nude mice. Tumors originating from MYBL2 knockdown cells exhibited slower growth compared to those from NC cells (Fig. 8A–C). We also noted a decrease in SMO protein expression in the shMYBL2 group, while an increase was observed in the MYBL2 group (Fig. 8D and E). Furthermore, lower Ki67 and SMO expressions were observed in the shMYBL2 group. Based on these results, MYBL2 promotes ccRCC tumorigenesis and enhances SMO expression in vivo (Fig. 8F).

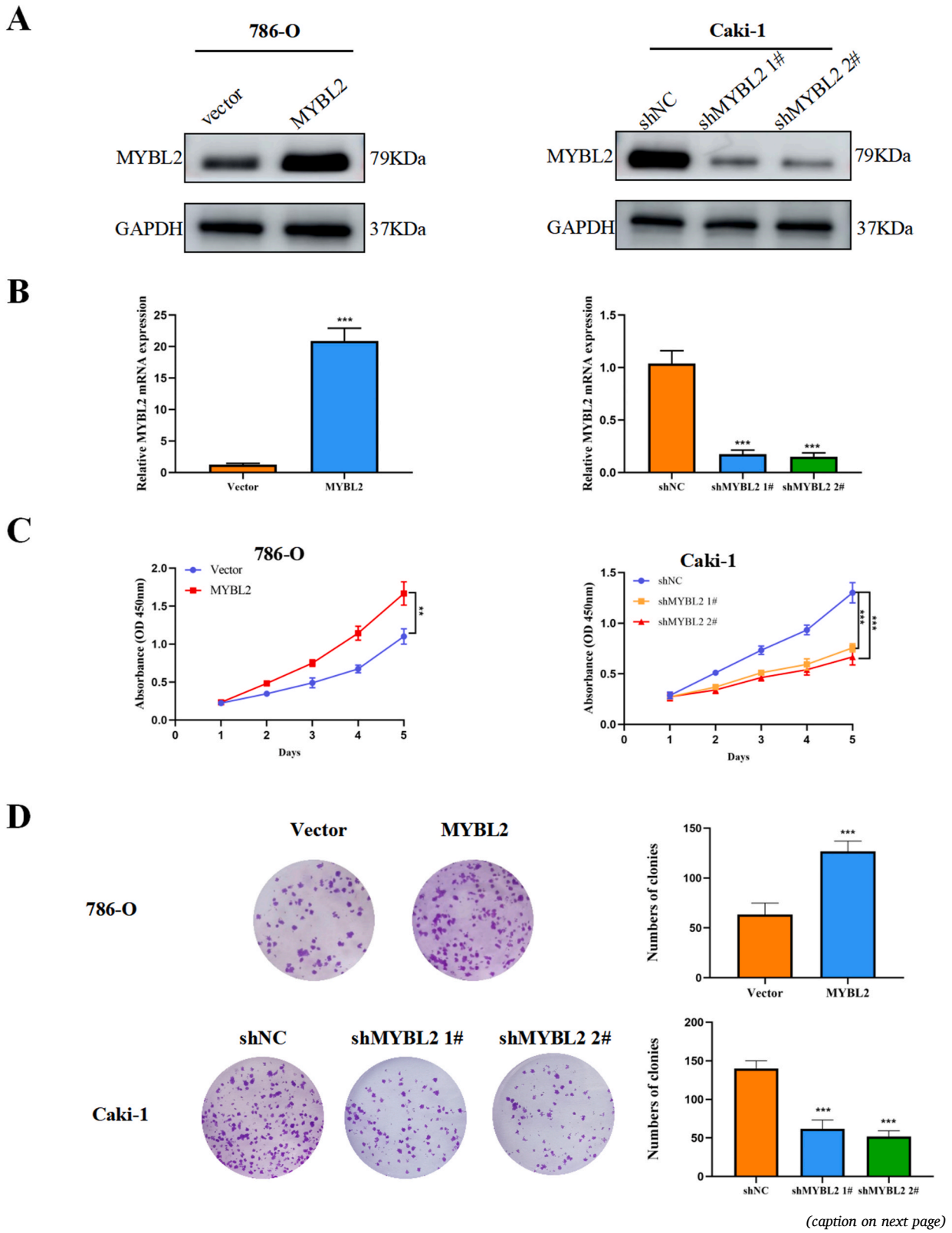

(caption on next page)

Fig. 3. MYBL2 has potent oncogenic functions in RCC. Caki-1 cells transfected with shRNA targeting MYBL2 were designated as shMYBL2, while cells transfected with empty lentiviral vectors served as negative controls (shNC). 786-O cells were transfected with lentiviruses overexpressing MYBL2, designated as MYBL2, with cells transfected with empty lentiviral vectors serving as controls (Vector). Validation of MYBL2 expression was conducted through Western blot analysis (A) and qRT-PCR (B). The CCK-8 assay results (C) depict the effects on cell viability of Caki-1 and 786-O cells following silencing or overexpression of MYBL2. Colony formation assay results (D) illustrate the impact on colony formation of Caki-1 and 786-O cells after knockdown or overexpression of MYBL2. The data are presented as the mean ± standard deviation (SD) of experiments (n = 3 biological replicates). *p < 0.05, **p < 0.01, ***p < 0.001.

3. Discussion

Despite improvements in diagnosing and treating ccRCC patients, statistical analysis shows that the five-year overall survival rate has remained unsatisfactorily low over the past few decades. Targeted drugs and immunotherapy offer innovative approaches for treating ccRCC. However, their efficacy is hampered by adverse side effects and acquired resistance, limiting their effectiveness to only 30% of the patient population.

The development and progression of tumors hinge on the interplay between cell-autonomous and cell-non-autonomous mechanisms. MYBL2, a reported driver in various malignancies, significantly influences this process. A study by Liu W et al. on bladder cancer, for instance, found that the absence of MYBL2 halted cell proliferation and migration, while its overexpression had the contrary effect [19]. Moreover, MYBL2 functions as a key transcription factor of CDCA8, heightening its expression that invariably escalates chemoresistance and aggressiveness in ovarian cancer [20]. Sun et al.'s prior study indicated that the upregulation of MYBL2 independently predicted a poorer prognosis in ccRCC patients [21]. Our investigation unveiled a substantial increase in MYBL2 levels in most ccRCC cell lines and tumor samples, in contrast to normal kidney cells and adjacent tissues. Furthermore, elevated MYBL2 levels were linked with higher postoperative recurrence rates and decreased overall survival in ccRCC patients. Experimental evidence also indicated that MYBL2 overexpression fosters tumor cell growth, both in the laboratory and in living organisms. Additionally, high MYBL2 expression might inhibit apoptosis by stimulating Bcl-xl and concurrently suppressing Bax expression. In-depth analysis of RNA sequencing data suggested that MYBL2 knockdown inhibits SMO expression, providing valuable insight into the complex function of MYBL2 in tumor progression.

The activity of MYBL2 is highly regulated at transcriptional levels [22,23]. Stimulation of the Akt/FOXM1 pathway markedly enhanced MYBL2 expression [24]. In addition, as a direct molecular motif kinase 1 (UHMK1) interaction partner, MYBL2 is enriched in the nucleus stimulated by UHMK1, and then regulates cell cycle progression [25]. Furthermore, investigations have been conducted on the interaction of MYBL2. Li et al. documented that MYBL2 might augment the castration-resistant growth of androgen-dependent prostate cancer cells by boosting the transcriptional activity of RACGAP1, a pivotal inhibitor of Hippo signaling [26]. MYBL2 is essential in colorectal cancer (CRC) for promoting DNA synthesis and cell cycle progression by binding directly to the RRM2 promoter [27]. In this research, a direct correlation was noted between MYBL2 and SMO expression. Furthermore, we provided evidence that MYBL2 directly interacts with the SMO promoter region, stimulating gene transcription. Beyond transcriptional control, epitranscriptomic RNA modifications also play a crucial role in gene regulation, influencing cancer progression [28,29]. A study by Xie et al. on bladder cancer demonstrated that N-acetyltransferase 10 (NAT10) binds and stabilizes AHNAK mRNA, protecting it from exonucleases and contributing to cisplatin resistance. Moreover, a multitude of tumor-associated immune cells, particularly tumor-associated macrophages and tumor-associated neutrophils, are recognized for their pivotal role in cancer metastasis [30]. Whether MYBL2 possesses the aforementioned functions affecting the occurrence, development, and drug resistance of ccRCC, further experimental verification is needed.

The Hedgehog (HH) signaling pathway, a frequently observed oncogenic mechanism, is significantly activated in patients with initial-stage RCC. Numerous investigations have further unveiled that abnormal HH signaling has strong associations with tumor dimensions, tumor angiogenesis, and the stemness of cancer cells. This aberration is also indicative of an elevated likelihood of lymph node metastasis and higher postoperative recurrence rates [31–33]. Under normal circumstances, when the HH signaling pathway is in action, HH ligands engage with PTCH1. This connection lifts the suppressive effect of PTCH on SMO, instigating the downstream translocation of GLI molecules that promote tumor growth. Thus, SMO emerges as a crucial target in cancer therapy [34–36]. Elevated PTCH levels and decreased SMO expression are key indicators linked to better survival rates in ccRCC patients [37]. However, the mechanism underlying MYBL2's regulation of the HH signaling pathway remains elusive. This research revealed a strong connection between the expression patterns of MYBL2 and SMO. Furthermore, SMO gene silencing partially reversed the proliferative and anti-apoptotic abilities of MYBL2 in cells. Bai et al. revealed that HOTAIR would promote tumor angiogenesis and increasing cancer stemness in RCC. They also found a critical link between HOTAIR and the Hedgehog pathway, particularly with GLI2. In fact, they discovered that HOTAIR interacts directly with AR, and they can cooperatively bind to the GLI2 promoter, thereby enhancing its transcription activity [38]. Regardless of these significant findings, research regarding the role of the Hedgehog pathway in ccRCC still lags in comparison to studies on other malignant tumors.

This study has certain limitations. Initially, our investigation primarily focuses on the influence of MYBL2 on the proliferation and apoptosis in ccRCC. However, existing research indicates that MYBL2 is implicated in promoting tumor cell migration and drug resistance [39,40]. Subsequent studies will delve into an in-depth exploration of MYBL2's involvement in the migration of ccRCC and its resistance to sunitinib. Additionally, earlier research has demonstrated that MYBL2 derived from tumors transcriptionally activates CCL2, leading to the recruitment of M2-like macrophages in both clinical tumor tissues and model mice [41]. This finding underscores the correlation between MYBL2 and immune infiltrates in cancer. Our next step involves collecting additional tissue samples from ccRCC patients undergoing immunotherapy, with the aim of further clarifying MYBL2's role in immunotherapeutic approaches for

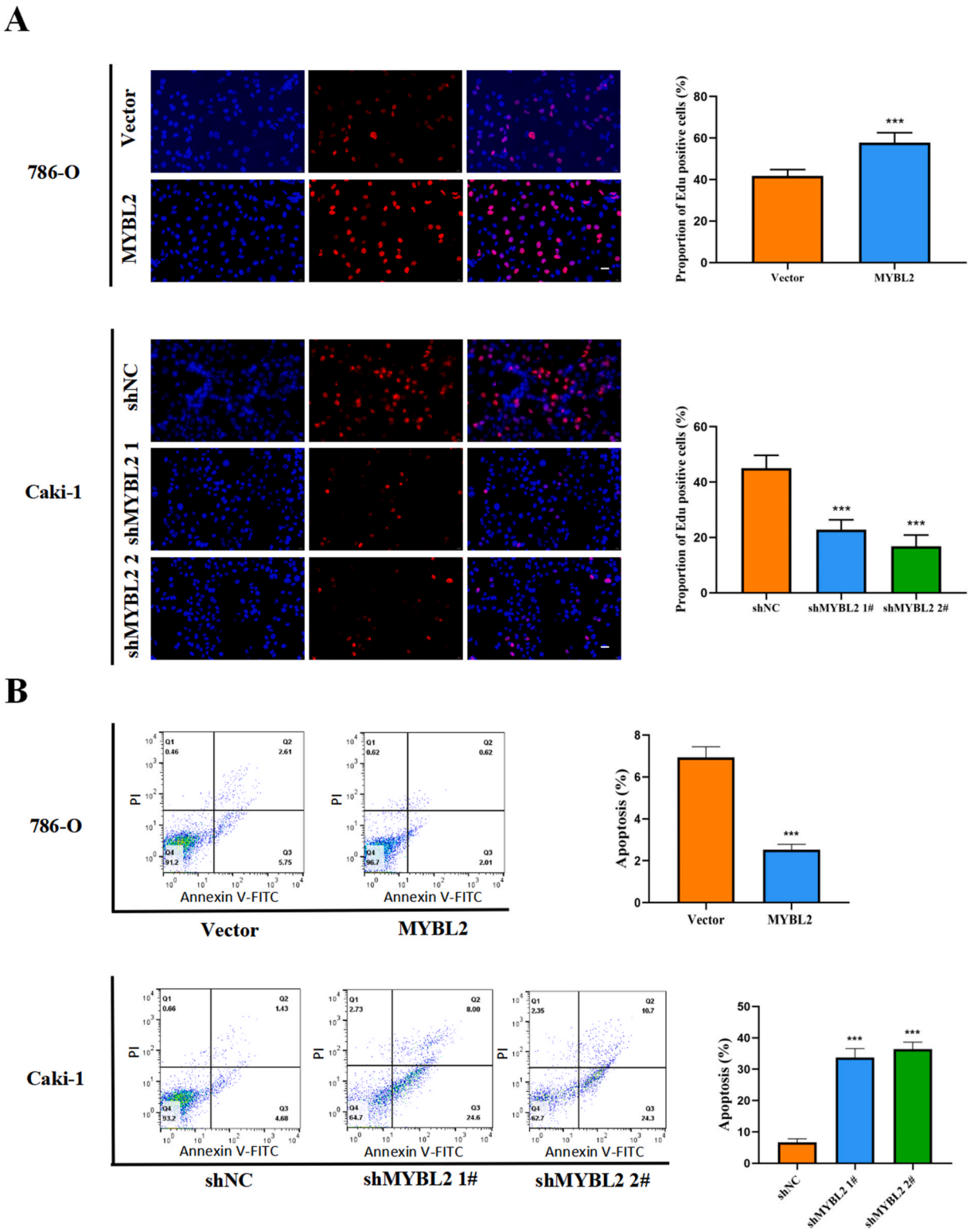

Fig. 4. MYBL2 has potent oncogenic functions in RCC. (A) The EdU assay was employed to evaluate the proliferation of Caki-1 and 786-O cells after MYBL2 knockdown or overexpression. Scale bar = 50 μm. (B) Flow cytometry was utilized to determine the apoptosis rate of Caki-1 and 786-O cells following MYBL2 knockdown or overexpression. The data are presented as the mean ± standard deviation (SD) of experiments (n = 3 biological replicates). *p < 0.05, **p < 0.01, ***p < 0.001.

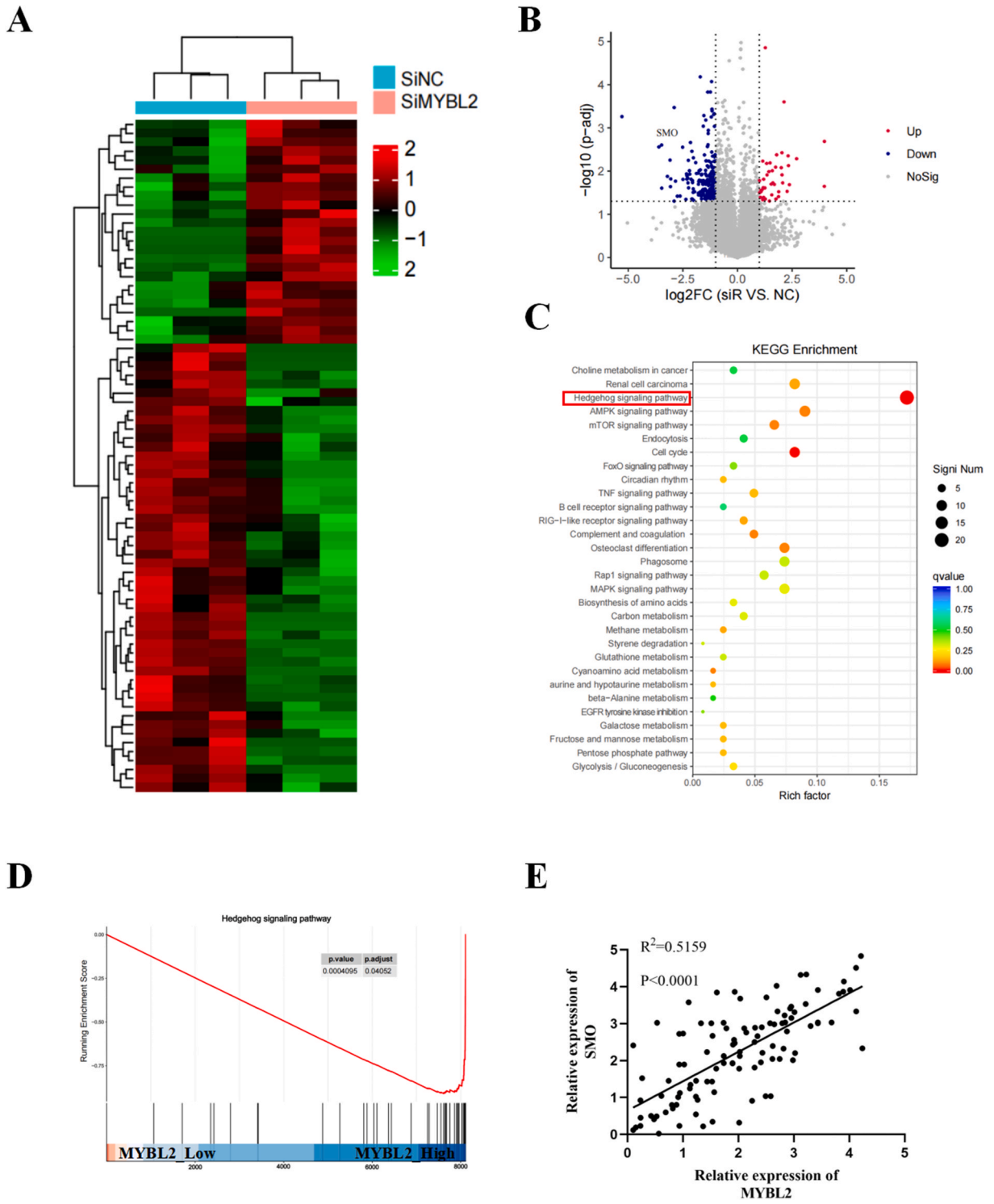

Fig. 5. SMO expression is closely related to MYBL2 expression in vitro. (A) Heatmap illustrating the Differentially Expressed Genes (DEGs) in the MYBL2 silenced (shMYBL2) and negative control (shNC) groups. DEGs with a log2 fold change (FC) > 1 are depicted in red, while those with a log2 FC < 1 are shown in green. (B) Volcano plot displaying the DEGs in the shMYBL2 and shNC groups of Caki-1 cells. (C) Kyoto Encyclopedia of Genes and Genomes (KEGG) analysis revealing the primary signaling pathways participated in by the DEGs. (D) Gene set enrichment analysis (GSEA) of the RNA-seq data indicating the suppression of the Hedgehog signaling pathway following MYBL2 silencing. (E) Positive correlation in the expression patterns of MYBL2 and SMO observed in RCC specimens. The data are presented as the mean ± standard deviation (SD) of experiments (n = 3 biological replicates). *p < 0.05, **p < 0.01, ***p < 0.001.

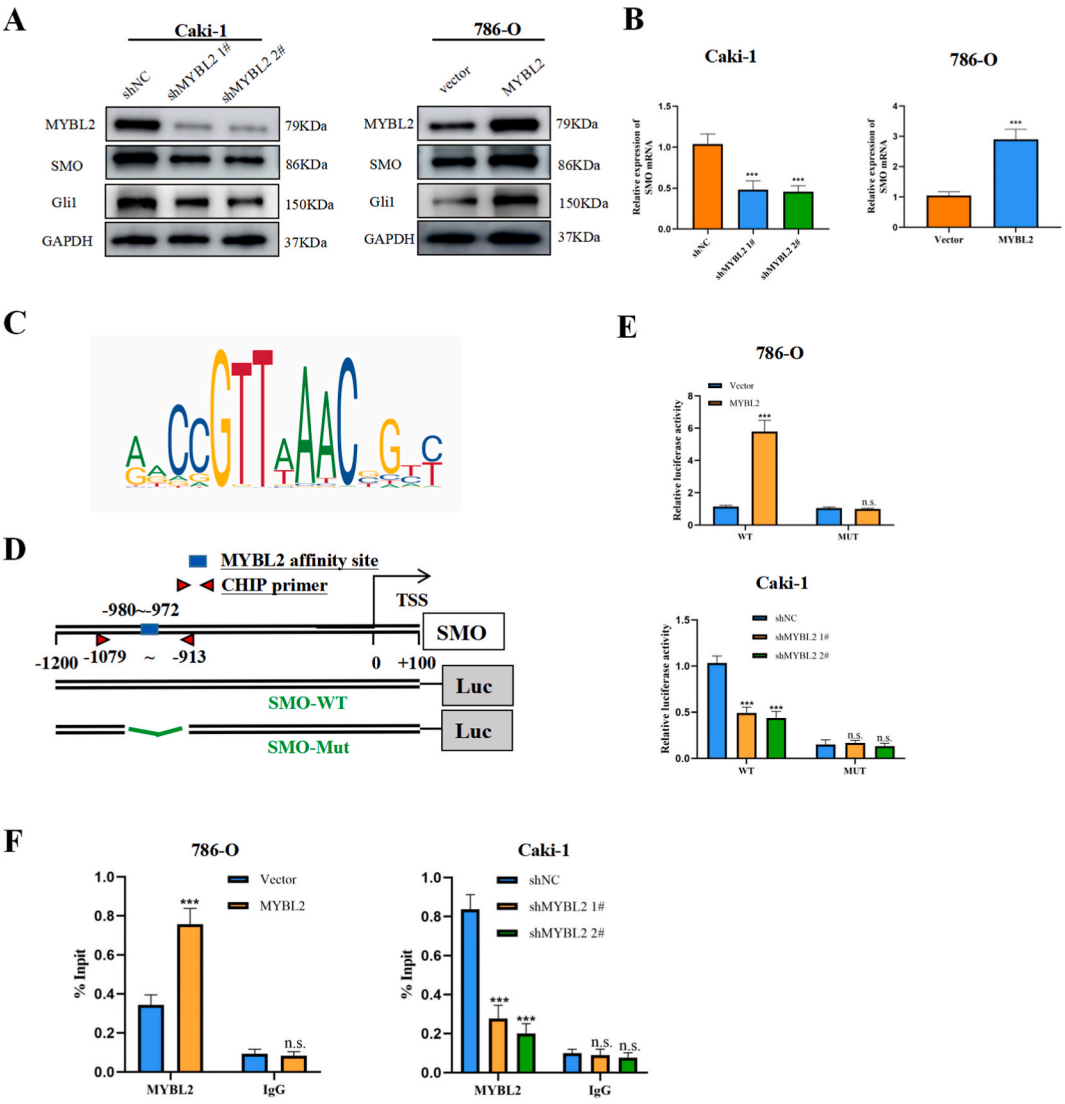

Fig. 6. SMO expression level was regulated by MYBL2. (A) SMO expression was evaluated by Western blot analysis. (B) qRT-PCR was performed to assess SMO expression levels. (C) The binding site of MYBL2 was retrieved from the JASPAR database. (D) Diagram depicting the predicted binding site of MYBL2 on the SMO promoter, along with primers for ChIP-qPCR and design of wild-type/mutant SMO promoter plasmids. (E) Quantification of luciferase activity in cells transfected with the MYBL2 promoter reporter. (F) Evaluation of MYBL2 enrichment on the SMO gene promoter using ChIP analysis, with IgG serving as a negative control. The data are presented as the mean ± standard deviation (SD) of experiments (n = 3 biological replicates). *p < 0.05, **p < 0.01, ***p < 0.001.

ccRCC.

In summary, our findings demonstrate that MYBL2 governs the transcription of SMO. Consequently, this contributes to the malignant characteristics observed in ccRCC cells. According to these results, MYBL2 may be a potential target for future ccRCC treatments.

4. Materials and methods

4.1. Tissue specimens

Approval for the study protocol was granted by the Research Ethics Committee at Peking Union Medical College Hospital. Informed consent was obtained from all individuals. The ccRCC and corresponding paracancerous tissues were collected post partial or radical nephrectomy, with histological confirmation of their nature.

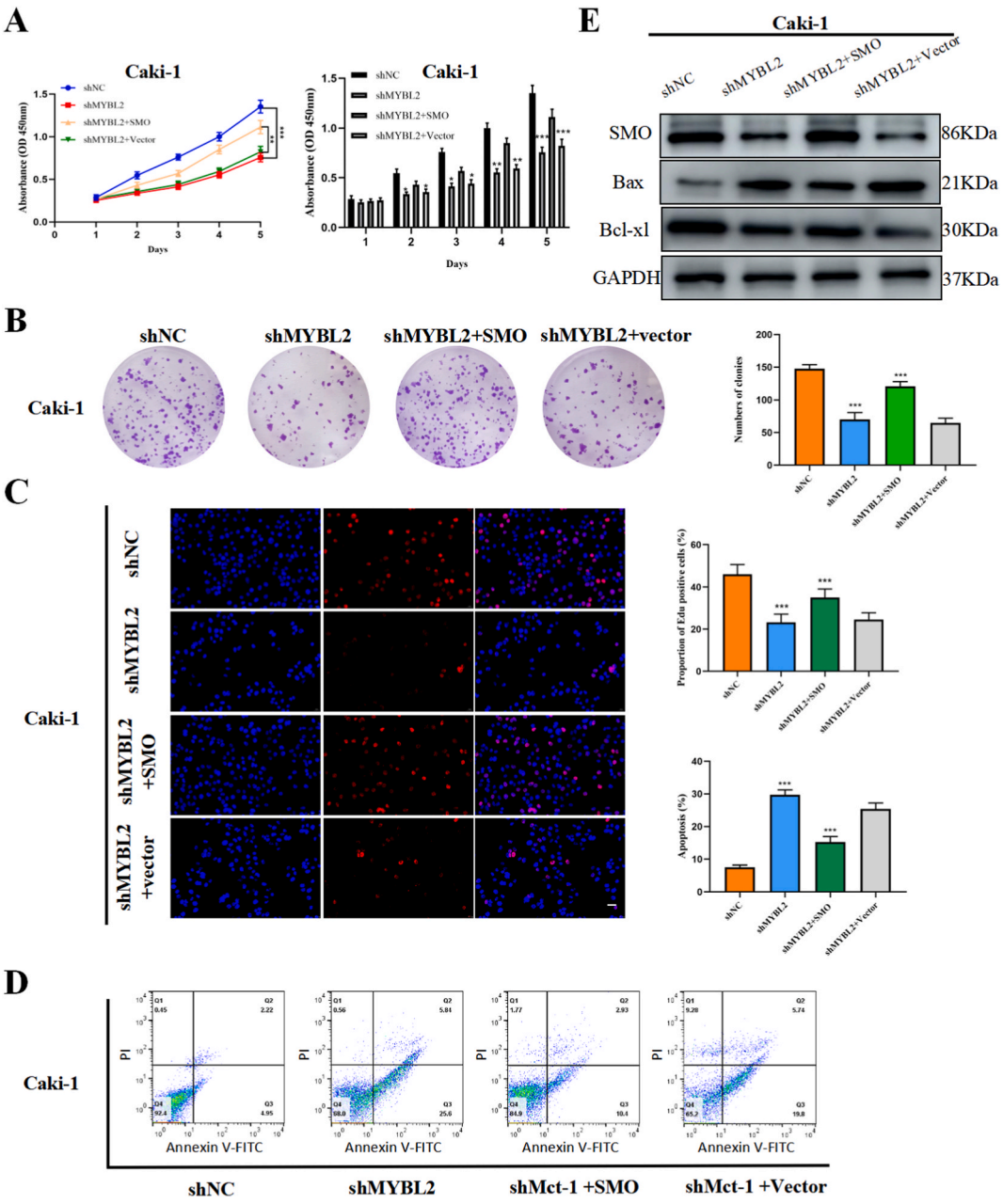

Fig. 7. MYBL2 influenced ccRCC proliferation and apoptosis by transactivating SMO. (A–D) Analysis of CCK-8, colony formation, EdU, and cell apoptosis in MYBL2-knockdown Caki-1 cells transfected with the SMO plasmid or vector. Scale bar = 50 μm. (E) Protein expression of SMO, along with the anti-apoptotic proteins Bax and Bcl-xl, in Caki-1 cells transfected with the MYBL2 knockdown lentivirus (shMYBL2) and SMO-overexpression plasmid. Scale bar = 50 μm. The data are presented as the mean ± standard deviation (SD) of experiments (n = 3 biological replicates). *p < 0.05, **p < 0.01, ***p < 0.001.

4.2. Cells culture

The human ccRCC cell lines 769-P, 786-O, Caki-1, Caki-2, and ACHN, along with human renal epithelial cell lines HK-2 and 293T cells, were obtained from the American Type Culture Collection (Manassas, VA, USA). Dulbecco's modified Eagle's medium supplemented with 10% fetal bovine serum and 100 mg/mL penicillin/streptomycin was used as a culture medium. The cells were cultured in humidified incubators with 5% CO2 at 37 °C.

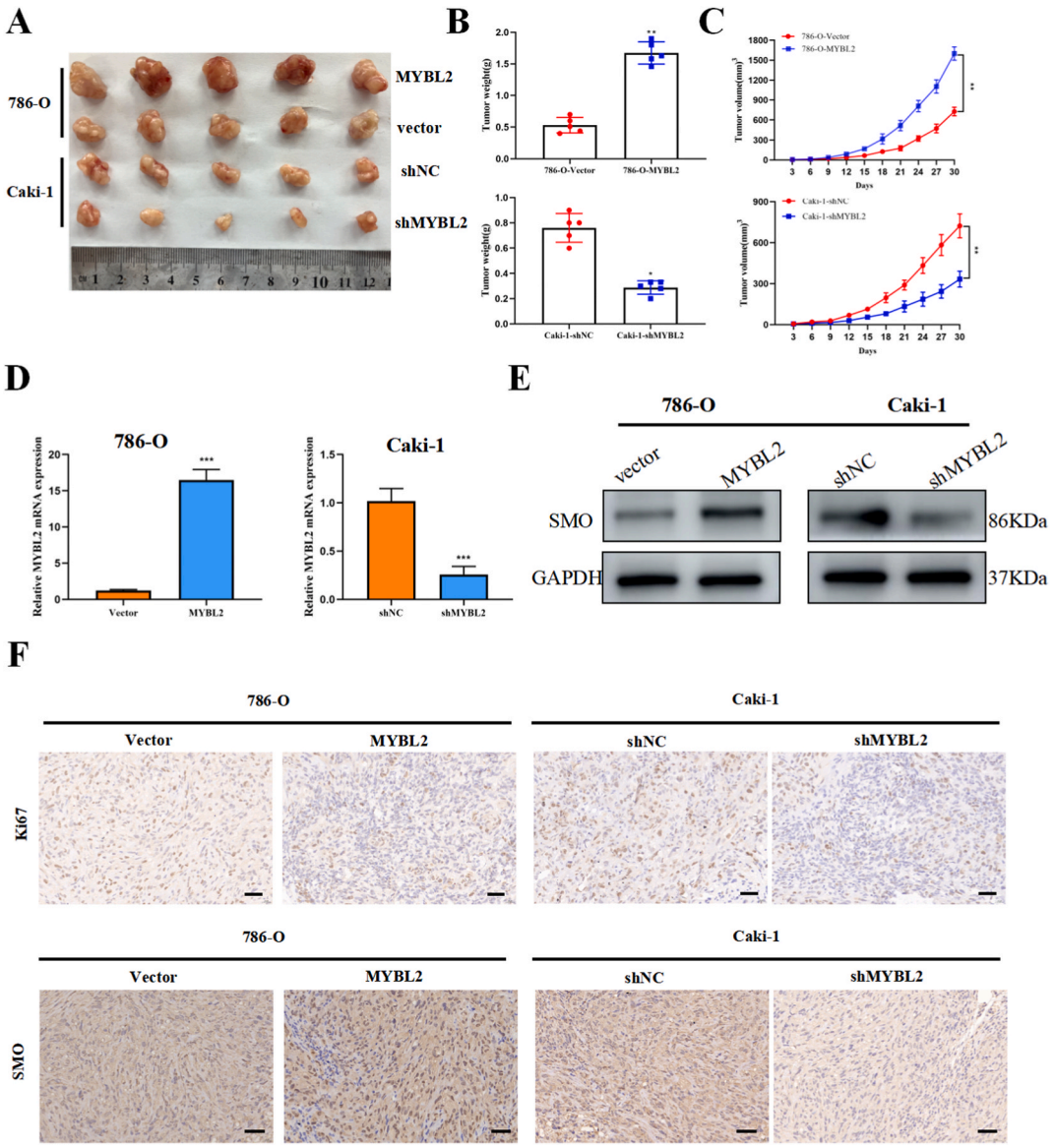

Fig. 8. MYBL2 upregulation contributed to RCC progression in vivo. (A–C) Representative images of tumors originating from lentivirus-mediated MYBL2-silenced Caki-1 cells and MYBL2-overexpressing 786-O cells. Tumor volume and weight were measured. (D) Analysis of MYBL2 expression levels in the xenografts by qRT-PCR. (E) Detection of SMO expression levels in xenografts by Western blot analysis. (F) Immunostaining images showing the expression levels of Ki-67 and SMO in xenografts. Scale bar = 50 μm. The data are presented as the mean ± standard deviation (SD) of experiments (n = 3 biological replicates). *p < 0.05, **p < 0.01, ***p < 0.001.

4.3. Western blot analysis

Cell lines or tissues were centrifuged at 14,000 g for 15 min at 4 °C after being extracts with RIPA lysis buffer. SDS-PAGE was used to separate the proteins and PVDF membrane was used to transfer them. In this investigation, the following primary antibodies were utilized: MYBL2 (ab238825, Abcam, 1:1000), SMO (ab52771, Abcam, 1:1000), Bax (ab32503, Abcam, 1:1000), Bcl-xl (ab32124, Abcam, 1:1000), and GAPDH (ab8245, Abcam, 1:1000); Protein signals were detected using a chemiluminescence kit from Bio-Rad.

4.4. Quantitative reverse transcription-polymerase chain reaction (qRT-PCR)

The manipulations were carried out as previously described. The results were calculated using the $2^{-\Delta\Delta CT}$ method. We used the following primers to amplify the target mRNA and internal control mRNA: MYBL2 forward (5′-CTTGAGCGAGTCCAAAGACTG-3′) and reverse (5′-AGTTGGTCAGAAGACTTCCCT-3′); SMO forward (5′-GCTCTTACTGACTGGCATGAG-3′) and reverse: (5′-

GAGTCATGACTCCTCGGATGAGG-3′) and GAPDH forward (5′-GGAGCGAGACCCTCCAAAAT-3′) and reverse (5′-GGCTGTTGTCA-TACTTCTCAT GG-3′).

4.5. Cell transfection

To establish stable cell lines, both Caki-1 and 786-O cell lines were transfected with lentiviruses containing MYBL2 knockdown, a negative control (shMYBL2/shNC), MYBL2 overexpression, or scrambled sequences (MYBL2/Vector) provided by GenePharma (Shanghai, China). Following is the sequence of shRNAs: 5′-GCCAUGGACCAAAGAGGAATT-3' (shMYBL2-1), 5′-CCUUCCUG-GAUUCCUG-UAATT-3' (shMYBL2-2). siRNA and plasmid transfection SMO expression vectors were also synthesized by GenePharma. According to the product manual, Lipofectamine 3000 Transfection Reagent was used to transfect the cells with SMO cDNA and siRNA.

4.6. Cell viability assay

Add 100 μl of PBS to each well in the outermost row of a 96-well plate. Then, seed tumor cells into the 96-well plate, with each well containing 100 μl of medium containing 1000 cells. After 24 h, add 10 μl of CCK-8 reagent (Dojindo, Japan) to each well. Following the 2-h incubation period, under conditions avoiding light, measure the absorbance at 450 nm using a spectrophotometer, and record the daily changes in cell absorbance.

4.7. Colony formation assay

The Caki-1 and 786-O cells, stably transfected, were seeded in six-well plates at a density of 1000 cells per well. Cultured in DMEM containing 10% fetal bovine serum (FBS) for two weeks, the colonies were harvested, fixed in 4% paraformaldehyde for 15 min, and stained with 0.1% crystal violet.

4.8. The 5-ethynyl-2′-deoxyuridine (Edu) proliferation assay

A total of 2×10^5 cells were cultured in a 12-well plate for 24 h. Subsequently, they were treated with 2% glycine and 0.5% Triton X-100 for 30 min, followed by staining with Apollo staining reaction buffer for 30 min and DAPI for 15 min. Fluorescence microscopy was employed to assess the EdU incorporation rate.

4.9. Flow cytometry assay

Flow cytometry and Annexin V staining were employed to assess apoptosis following the manufacturer's instructions. Briefly, 5×10^5 cells were harvested, washed twice with assay buffer, and analyzed by flow cytometry after extraction.

4.10. Immunohistochemical (IHC) analysis

The xenografts and ccRCC tissues were fixed in formalin and embedded in paraffin. The manufacturer's instructions were followed when staining paraffin-embedded tissue sections. Two experienced pathologists independently evaluated and graded the MYBL2, SMO, and Ki67 expression levels. The proportions of positive tumor cells were assessed based on the following criteria: score 0 (0%–5%), score 1 (6%–25%), score 2 (26%–50%), score 3 (51%–75%), and score 4 (>75%). These criteria were also utilized to grade the intensity of protein staining: score 0 (negative staining), score 1 (weak staining - light yellow), score 2 (moderate staining - yellow-brown), and score 3 (strong staining - brown). Based on the staining intensity score multiplied by the percentage of positive tumor cells, the staining index (SI) was calculated.

4.11. Luciferase reporter assay

In brief, the promoter sequences of SMO-WT and SMO-MUT were cloned into a pGL3-promoter vector. We co-transfected luciferase reporter plasmids with 10 ng of pRL-TK Renilla plasmids into 293T cells. The luciferase activity was measured following a 48-h incubation period.

4.12. Chromatin immunoprecipitation (CHIP) assay

The ChIP assay was conducted according to the manufacturer's instructions using the Beyotime Chromatin Immunoprecipitation kit (Cell Signaling Technology, Danvers, MA, USA). The ChIP DNA underwent amplification via qRT-PCR. The sequences for SMO promoter were as follows: SMO forward, (5′-TAGTCCTTCCTACCCCAATTTCC-3′); SMO reverse, (5′-TTGGTCCTTAGCCACTCCTTC-3′).

4.13. Tumor xenograft models

Twenty male BALB/c nude mice aged 4 weeks old and weighing 18-20 g were purchased from the Laboratory Animal Resources Center of Peking Union Medical College and allocated them randomly into four groups: Caki-1-shMYBL2/shNC, and 786-O-MYBL2/

vector. In the xenograft model, 2×10^6 cells suspended in 100 μL PBS per mouse were subcutaneously injected into the dorsal flank. After fixing in 4% paraformaldehyde, all samples were stained by immunohistochemistry.

4.14. Statistical analysis

In this study, mean and standard deviation (SD) were calculated using GraphPad Prism 8 and SPSS 20.0. Student's t-tests were used to determine differences between the means. All log-rank tests and survival analyses were conducted using the Kaplan-Meier method. Statistical significance was defined as $p < 0.05$ for all analyses.

Funding

This work was supported by the Chinese Academy of Medical Sciences Innovation Fund for Medical Sciences (2022-I2M-1-008) and the National High Level Hospital Clinical Research Funding (2022-PUMCH-B-008).

Ethics approval statement

The Animal Care and Use Committees of Peking Union Medical College Hospital [institutional approval number for lab animal studies: XHDW-2022-073] were performed in accordance with the ethical standards laid down in The Declaration of Helsinki. The present study was conducted with written informed consent from all of the patients.

Availability of data and materials

All data generated or analyzed during this study are included in this published article.

CRediT authorship contribution statement

Wenjie Yang: Formal analysis, Data curation. **Hualin Chen:** Methodology, Investigation. **Lin Ma:** Data curation, Conceptualization. **Mengchao Wei:** Formal analysis. **Xiaoqiang Xue:** Software. **Yingjie Li:** Methodology. **Zhaoheng Jin:** Data curation. **Jie dong:** Writing – original draft. **He Xiao:** Writing – original draft.

Declaration of competing interest

The authors declare that they have no known competing financial interests or personal relationships that could have appeared to influence the work reported in this paper.

Appendix A. Supplementary data

Supplementary data to this article can be found online at https://doi.org/10.1016/j.heliyon.2024.e27772.

References

[1] R.L. Siegel, K.D. Miller, H.E. Fuchs, A. Jemal, Cancer statistics, 2022, CA Cancer J Clin 72 (1) (2022) 7–33.
[2] A. Mejean, A. Ravaud, S. Thezenas, S. Colas, J.B. Beauval, K. Bensalah, et al., Sunitinib alone or after nephrectomy in metastatic renal-cell carcinoma, N. Engl. J. Med. 379 (2018) 417–427.
[3] U. Capitanio, K. Bensalah, A. Bex, S.A. Boorjian, F. Bray, J. Coleman, et al., Epidemiology of renal cell carcinoma, Eur. Urol. 75 (2019) 74–84.
[4] S. Turajlic, C. Swanton, C. Boshoff, Kidney cancer: the next decade, J. Exp. Med. 215 (2018) 2477–2479.
[5] I.B. Riaz, H. He, A.J. Ryu, R. Siddiqi, S.A.A. Naqvi, Y. Yao, et al., A living, interactive systematic review and network meta-analysis of first-line treatment of metastatic renal cell carcinoma, Eur. Urol. 80 (2021) 712–723.
[6] J. Schodel, S. Grampp, E.R. Maher, H. Moch, P.J. Ratcliffe, P. Russo, et al., Hypoxia, hypoxia-inducible transcription factors, and renal cancer, Eur. Urol. 69 (2016) 646–657.
[7] K. Morita, S. He, R.P. Nowak, J. Wang, M.W. Zimmerman, C. Fu, et al., Allosteric activators of protein phosphatase 2A display broad antitumor activity mediated by dephosphorylation of MYBL2, Cell 181 (2020) 702–715.
[8] R. Bayley, C. Ward, P. Garcia, MYBL2 amplification in breast cancer: molecular mechanisms and therapeutic potential, Biochim. Biophys. Acta Rev. Canc 1874 (2020) 188407.
[9] X. Chen, Y. Lu, H. Yu, K. Du, Y. Zhang, Y. Nan, et al., Pan-cancer analysis indicates that MYBL2 is associated with the prognosis and immunotherapy of multiple cancers as an oncogene, Cell Cycle 20 (2021) 2291–2308.
[10] Y. Ciciro, A. Sala, MYB oncoproteins: emerging players and potential therapeutic targets in human cancer, Oncogenesis 10 (2021) 19.
[11] N. Takebe, L. Miele, P.J. Harris, W. Jeong, H. Bando, M. Kahn, et al., Targeting Notch, Hedgehog, and Wnt pathways in cancer stem cells: clinical update, Nat. Rev. Clin. Oncol. 12 (2015) 445–464.
[12] J. Briscoe, P.P. Therond, The mechanisms of Hedgehog signalling and its roles in development and disease, Nat. Rev. Mol. Cell Biol. 14 (2013) 416–429.
[13] N.G. Steele, G. Biffi, S.B. Kemp, Y. Zhang, D. Drouillard, L. Syu, et al., Inhibition of Hedgehog signaling alters fibroblast composition in pancreatic cancer, Clin. Cancer Res. 27 (2021) 2023–2037.
[14] J. Jiang, Hedgehog signaling mechanism and role in cancer, Semin. Cancer Biol. 85 (2022) 107–122.

[15] S. Wang, Y. Wang, X. Xun, C. Zhang, X. Xiang, Q. Cheng, et al., Hedgehog signaling promotes sorafenib resistance in hepatocellular carcinoma patient-derived organoids, J. Exp. Clin. Cancer Res. 39 (2020) 22.
[16] I.A.A. Ruiz, Hedgehog signaling and the Gli code in stem cells, cancer, and metastases, Sci. Signal. 4 (200) (2011) pt9.
[17] Y. Kong, Y. Peng, Y. Liu, H. Xin, X. Zhan, W. Tan, Twist1 and Snail link Hedgehog signaling to tumor-initiating cell-like properties and acquired chemoresistance independently of ABC transporters, Stem Cell. 33 (4) (2015) 1063–1074.
[18] C. Tang, L. Li, Q. Xu, S. Xu, et al., ACKR3 orchestrates Hedgehog signaling to promote renal cell carcinoma progression, Mol. Carcinog. 62 (6) (2023) 882–893.
[19] W. Liu, D. Shen, L. Ju, R. Zhang, W. Du, W. Jin, et al., MYBL2 promotes proliferation and metastasis of bladder cancer through transactivation of CDCA3, Oncogene 41 (2022) 4606–4617.
[20] G. Qi, C. Zhang, H. Ma, Y. Li, J. Peng, J. Chen, et al., CDCA8, targeted by MYBL2, promotes malignant progression and olaparib insensitivity in ovarian cancer, Am. J. Cancer Res. 11 (2021) 389–415.
[21] S.S. Sun, Y. Fu, J.Y. Lin, Upregulation of MYBL2 independently predicts a poorer prognosis in patients with clear cell renal cell carcinoma, Oncol. Lett. 4 (2020) 2765–2772.
[22] F. Zhong, T. Chen, B. Li, Combinatorial transcriptional regulation of HEB/ZEB1/ASCL1 and MYBL2 on Ras/ErbB signaling, Biochem. Biophys. Res. Commun. 622 (2022) 170–176.
[23] O. Vera, I. Bok, N. Jasani, K. Nakamura, X. Xu, N. Mecozzi, et al., A MAPK/miR-29 Axis suppresses melanoma by targeting MAFG and MYBL2, Cancers 13 (6) (2021).
[24] X. Zhang, Q.L. Lv, Y.T. Huang, L.H. Zhang, H.H. Zhou, Akt/FoxM1 signaling pathway-mediated upregulation of MYBL2 promotes progression of human glioma, J. Exp. Clin. Cancer Res. 36 (2017) 105.
[25] T. Wei, S.M.E. Weiler, M. Toth, C. Sticht, T. Lutz, S. Thomann, et al., YAP-dependent induction of UHMK1 supports nuclear enrichment of the oncogene MYBL2 and proliferation in liver cancer cells, Oncogene 38 (2019) 5541–5550.
[26] Q. Li, M. Wang, Y. Hu, E. Zhao, J. Li, L. Ren, et al., MYBL2 disrupts the Hippo-YAP pathway and confers castration resistance and metastatic potential in prostate cancer, Theranostics 11 (2021) 5794–5812.
[27] Q. Liu, L. Guo, H. Qi, M. Lou, R. Wang, B. Hai, et al., A MYBL2 complex for RRM2 transactivation and the synthetic effect of MYBL2 knockdown with WEE1 inhibition against colorectal cancer, Cell Death Dis. 12 (2021) 683.
[28] R. Xie, L. Cheng, M. Huang, L. Huang, Z. Chen, Q. Zhang, et al., NAT10 drives cisplatin chemoresistance by enhancing ac4C-associated DNA repair in bladder cancer, Cancer Res. 10 (2023) 1666–1683.
[29] X. Chen, R. Xie, P. Gu, M. Huang, J. Han, W. Dong, et al., Long noncoding RNA LBCS inhibits self-renewal and chemoresistance of bladder cancer stem cells through epigenetic silencing of SOX2, Clin. Cancer Res. 4 (2019) 1389–1403.
[30] Q. Zhang, S. Liu, H. Wang, K. Xiao, J. Lu, S. Chen, et al., ETV4 mediated tumor-associated neutrophil infiltration facilitates lymphangiogenesis and lymphatic metastasis of bladder cancer, Adv. Sci. 10 (2023) e2205613.
[31] J. Feng, C. Wang, T. Liu, J. Li, L. Wu, Q. Yu, et al., Procyanidin B2 inhibits the activation of hepatic stellate cells and angiogenesis via the Hedgehog pathway during liver fibrosis, J. Cell Mol. Med. 23 (2019) 6479–6493.
[32] R. Zhu, O. Gires, L. Zhu, J. Liu, J. Li, H. Yang, et al., TSPAN8 promotes cancer cell stemness via activation of sonic Hedgehog signaling, Nat. Commun. 10 (2019) 2863.
[33] F. Ramadan, A. Fahs, S.E. Ghayad, R. Saab, Signaling pathways in Rhabdomyosarcoma invasion and metastasis, Cancer Metastasis Rev. 39 (2020) 287–301.
[34] D. Doheny, S. Sirkisoon, R.L. Carpenter, N.R. Aguayo, A.T. Regua, M. Anguelov, et al., Combined inhibition of JAK2-STAT3 and SMO-GLI1/tGLI1 pathways suppresses breast cancer stem cells, tumor growth, and metastasis, Oncogene 39 (2020) 6589–6605.
[35] X. Wu, S. Xiao, M. Zhang, L. Yang, J. Zhong, B. Li, et al., A novel protein encoded by circular SMO RNA is essential for Hedgehog signaling activation and glioblastoma tumorigenicity, Genome Biol. 22 (2021) 33.
[36] C. Espinosa-Bustos, J. Mella, J. Soto-Delgado, C.O. Salas, State of the art of Smo antagonists for cancer therapy: advances in the target receptor and new ligand structures, Future Med. Chem. 11 (2019) 617–638.
[37] A. Dunatov Huljev, N. Kelam, B. Benzon, V. Soljic, et al., Expression pattern of sonic Hedgehog, patched and smoothened in clear cell renal carcinoma, Int. J. Mol. Sci. 24 (10) (2023).
[38] J.Y. Bai, B. Jin, J.B. Ma, T.J. Liu, C. Yang, Y. Chong, et al., HOTAIR and androgen receptor synergistically increase GLI2 transcription to promote tumor angiogenesis and cancer stemness in renal cell carcinoma, Cancer Lett. 498 (2021) 70–79.
[39] Y.J. Hui, H. Chen, X.C. Peng, L.G. Li, M.J. Di, H. Liu, et al., Up-regulation of ABCG2 by MYBL2 deletion drives Chlorin e6-mediated photodynamic therapy resistance in colorectal cancer, Photodiagnosis Photodyn. Ther. 42 (2023) 103558.
[40] M. Wei, R. Yang, M. Ye, Y. Zhan, B. Liu, L. Meng, et al., MYBL2 accelerates epithelial-mesenchymal transition and hepatoblastoma metastasis via the Smad/SNAI1 pathway, Am. J. Cancer Res. 12 (5) (2022) 1960–1981.
[41] B. Pan, T. Wan, Y. Zhou, S. Huang, L. Yuan, Y. Jiang, et al., The MYBL2-CCL2 axis promotes tumor progression and resistance to anti-PD-1 therapy in ovarian cancer by inducing immunosuppressive macrophages, Cancer Cell Int. 23 (1) (2023) 248.